Image capture array with an organic light sensor

R. A. Street, M. Mulato, R. Lau, J. Ho, J. Graham, Z. Popovic, and J. Hor

Citation: Applied Physics Letters **78**, 4193 (2001); doi: 10.1063/1.1380733
View online: http://dx.doi.org/10.1063/1.1380733
View Table of Contents: http://scitation.aip.org/content/aip/journal/apl/78/26?ver=pdfcov
Published by the AIP Publishing

Image capture array with an organic light sensor

R. A. Street,[a] M. Mulato,[b] R. Lau, and J. Ho
Xerox PARC, 3333 Coyote Hill Road, Palo Alto, California 94304

J. Graham, Z. Popovic, and J. Hor
Xerox Research Center of Canada, 2660 Speakman Drive, Mississauga, Ontario L5K 2L1, Canada

(Received 27 December 2000; accepted for publication 30 April 2001)

A large-area image capture device using an organic sensor is reported. The 512×512 pixel array, with 100×100 micrometer pixel size, combines amorphous silicon matrix addressing with a continuous organic sensor. The bilayer sensor comprises a tetraphenyldiamine hole transport layer on top of a benzimidazole perylene generator layer. This combination provides high sensitivity across the visible with low dark current. We present imaging properties and in particular show that the lateral charge transport between pixels is small, and that the effective fill factor is ~90%. X-ray imaging with a phosphor converter is demonstrated. © *2001 American Institute of Physics.* [DOI: 10.1063/1.1380733]

Digital image capture is generally achieved with charge coupled devices or complementary metal–oxide–semiconductor (CMOS) sensor arrays for digital camera applications, and with amorphous silicon (*a*-Si) arrays for large area x-ray imaging.[1] Organic electronic materials provide interesting new opportunities for both types of sensor.[2] For example, organic materials could replace the *a*-Si thin film transistors (TFT) and sensors in large area arrays and may also reduce manufacturing costs by using direct marking techniques such as jet printing.[3] The organic sensor thickness can be controlled over a wide range, allowing selection of the pixel capacitance, which is an important factor in the electronic noise.[1] The great variety of possible organic sensor materials allows the spectral response to be tuned to the emission of the x-ray conversion phosphor or for other selective imaging.

As an initial step towards demonstrating an entirely organic detector, we report an image sensor that combines *a*-Si addressing with an organic sensor. This device demonstrates the organic sensor performance in a pixel array that is manufacturable in a large area, and permits study of the critical interactions between neighboring pixels.

The device is an active matrix array of 512×512 square pixels of a 100×100 micrometer size. Pixel addressing uses *a*-Si TFT, and the fabrication of the switching matrix is discussed elsewhere.[1] Each pixel contains a TFT, a storage capacitor of ~0.4 pF, the address lines, and a contact pad to the sensor occupying 67% of the pixel area (the geometrical fill factor, F_G). Each pixel is separated from its neighbors by a silicon oxynitride insulator which also isolates the sensor from the underlying TFT and address lines. The insert to Fig. 1 illustrates a cross section view of the high fill factor design, in which the sensor is a continuous layer rather than patterned into individual pixel sensors.[4] This approach overcomes the difficulty of lithographic patterning of organic semiconductors, and offers the greatest possible sensor area. The continuous sensor design gives the possibility of undesired interactions between pixels, but we show that these effects are small.

The array is coated with the organic sensor with a two-layer structure.[5] First, a charge generation layer of benzimidazole perylene (BZP) is deposited by vacuum evaporation to a thickness of 300 nm. Next, a hole transport layer of tetraphenyldiamine (TPD) in a polycarbonate binder is spin coated to a thickness of about 10 μm. The TPD loading gives a hole mobility of about 10^{-5} cm^2/V s, without causing significant light scattering.[5] The two-layer structure is advantageous as the independent control over the generation and transport layers allows flexibility in the choice of thickness (and hence, pixel capacitance), single carrier charge collection and low dark current.

The sensor is coated with a Au/Pt semitransparent (35–45% transmittance) evaporated metal layer to provide the bias. The array is operated by external electronics which pro-

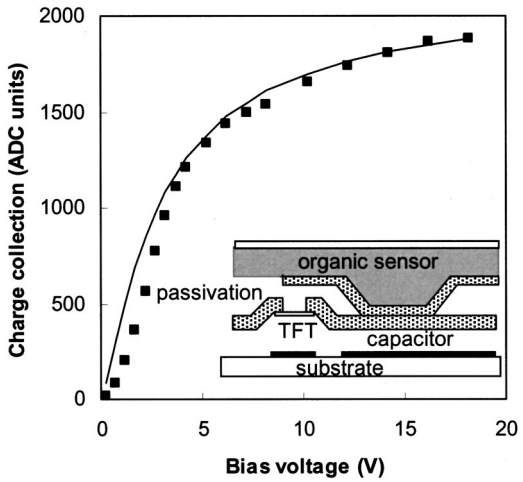

FIG. 1. The measured signal as a function of bias voltage (data points), and a plot of charge collection based on Eq. (1) (line), from which the mobility-lifetime product can be estimated. 1 ADC measurement unit corresponds to 800 electrons. The dark leakage current is about 7 ADC units and is subtracted from the signal. The insert shows the structure of the array pixel, with the TFT and the continuous sensor layer.

[a]Electronic mail: street@parc.xerox.com
[b]Present address; Departamento de Física e Matemática, Universidade de São Paulo, Ribeirão Preto, SP, 14040-901, Brasil.

vides signals to the TFT gates and transfers the signal charge to external amplifiers and a 14-bit analog-to-digital converter (ADC).[1] The electronics allows operation of the array at up to 20 Hz, with a 14-bit dynamic range and a minimum electronic noise of 1000–2000 electrons.

The sensor leakage current is a potential source of electronic noise and when large enough can also saturate the pixel storage capacitor. The room temperature leakage current for our device is below $0.2\,\mathrm{pA/mm^2}$ over the range of bias voltages used. This current corresponds to only 2 fC/pixel/s and is essentially negligible.

The choice of bias voltage is determined by the need for a high charge collection. Figure 1 shows the signal increasing with bias and approaching saturation, for illumination from a green light-emitting diode and a frame rate of 4 Hz. The solid line plots the well-known expression for charge collection, Q, in a film of thickness, d, at bias, V,[6]

$$Q/Q_0 = (\mu\tau V/d^2)[1-\exp(-d/\mu\tau V)], \tag{1}$$

where $\mu\tau$ is the mobility lifetime product, and has an assumed value of $\sim 2\times 10^{-7}\,\mathrm{cm^2/V}$, and Q_0 is the mobile charge generated by the illumination. The signal is a product of the generation efficiency and the charge collection, both of which are field dependent.[7] It is not easy to separate the two factors, but the fit to Eq. (1) suggests that $>85\%$ charge collection is achieved at 10 V bias. The transit time for holes is estimated to be $<10\,\mathrm{ms}$ at a 10 V bias, which is comfortably short enough for the frame rates used. Imaging at full video rate may require a shorter drift time, which is readily achieved by increasing the bias voltage. A long transit time causes significant image lag, in which charge is measured in the frames after the exposure. The image lag in the present array is $<10\%$.

The image sensor exhibits a spectral response across the visible spectrum extending from 400–800 nm, in agreement with the known spectrum of BZP.[7] The measured external quantum efficiency at 550 nm is $\sim 10\%$, consistent with an estimated 30% generation efficiency in the generator layer,[7] and the reflection losses in the semitransparent electrode. Indium tin oxide electrodes should enhance the external efficiency.

A successful image sensor also requires control of the signal cross talk between pixels due to the continuous sensor material. The spatial response was measured by imaging an illuminated slit much narrower than the pixel size, placed over the surface at a small angle to the pixel rows.[8] The result gives the line-spread function (LSF) and its Fourier transform is the modulation transfer function (MTF). Examples of the LSF using a slit width of 16 μm are shown in Fig. 2 for different illumination intensities. The LSF closely follows the pixel size, and the shoulders to the LSF show that no more than $\sim 10\%$ of the signal charge is transferred to neighboring pixels. The particular shape of the LSF identifies the mechanism as charge transport between the contact pads on adjacent pixels.[9] The plateau in the LSF shows that the lateral transfer of signal charge is approximately independent of where the illumination occurs on the pixel. This result is expected for conduction between the metal contact pads, because the potential on the pad is spatially invariant. However, optical or electrical cross talk arising within the sensor itself would be expected to have a strong dependence on the illumination position, for cross-talk mechanisms of diffusion, light scattering, or lateral drift.

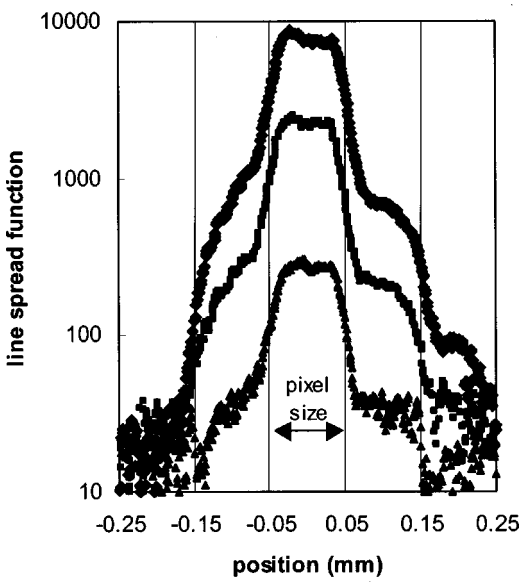

FIG. 2. The LSF of the array, measured at different illumination intensities in the range $0.1-5\ \mu\mathrm{W/cm^2}$.

The MTF as a function of spatial frequency, u, approximates to the $\mathrm{sinc}(\pi u d)$ form expected for a perfectly rectangular LSF defined by the pixel size, d. The measured MTF at the Nyquist frequency ($5\,\mathrm{mm^{-1}}$) is 0.6 ± 0.05, compared to the ideal value of 0.64. However, the first zero of the MTF is at $\sim 11\,\mathrm{mm^{-1}}$ rather than $1/d$ ($=10\,\mathrm{mm^{-1}}$), and suggests incomplete charge collection between the pixels. Such an effect is obviously plausible because charge collection in the gap between pixels occurs by a smaller lateral field to the adjacent contact pad, rather than by the vertical field when charge is collected over the pad (see Fig. 1). The charge collection in the gap was measured using the imaged slit data, by integrating the signal perpendicular to the slit for different positions of the slit on the pixel. The data in Fig. 3 shows that the total signal developed for illumination in the center of the gap decreases to about 70% of the value over the contact pads. The width of the slit is comparable to the

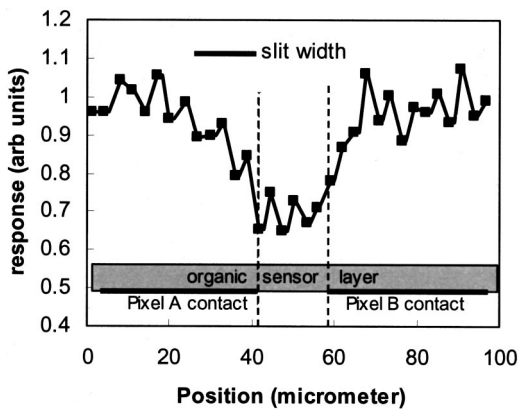

FIG. 3. Measurement of total signal charge as the illumination slit changes position between the centers of two adjacent pixels, showing lower sensitivity for illumination in the gap between the pixels. The figure illustrates the configuration of the pixel contact pads and the vertical lines indicate the location of the gap separating the adjacent pixels.

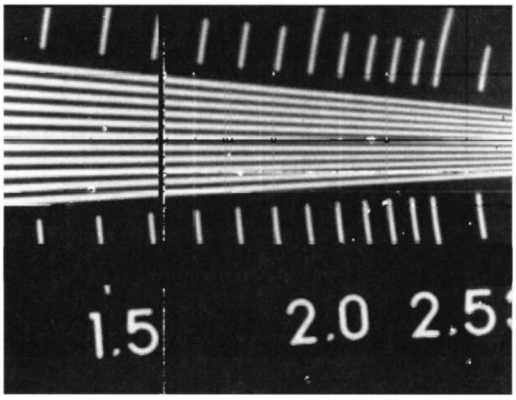

FIG. 4. X-ray image of a resolution target, acquired with a single radiographic x-ray exposure at 70 kVp, using a GdO_2S_2:Tb (Lanex Regular) phosphor placed on top of the array.

width of the gap, and so the measurement is a convolution of the gap response with the slit width. The lower charge collection in the gap reduces the effective fill factor, F_E, to an amount given by,

$$F_E = F_G + 0.7(1 - F_G), \tag{2}$$

which is roughly 90% for the present array. Thus, the continuous organic sensor film substantially increases the sensitivity of the array compared to a patterned pixel array, without significant reduction of spatial resolution, as evident from the minimal broadening of the LSF.

The ultimate test of an image sensor is the detection of images and an example is shown in Fig. 4. This is an x-ray image of a resolution target acquired at radiographic energies using a GdO_2S_2:Tb phosphor placed directly on the surface of the array. The phosphor emission is centered at 550 nm, well within the spectral response of the sensor. The numbers show the spatial resolution in mm^{-1} and the slight blurring of the image is entirely due to the phosphor, which has an MTF of ~ 0.2 at $3\,mm^{-1}$. Visible images, including color imaging by sequential capture of the three-color separations, have also been demonstrated.

In summary, the organic sensor has low leakage, high charge collection, and sensitivity across the visible spectrum. Successful integration with large area matrix addressing gives a high fill factor array, with good spatial resolution. All the indications are that the approach would be similarly successful with CMOS sensors.

The authors are grateful to members of the Xerox PARC process line for fabrication of arrays, and for support from the NIST ATP Program (70NANB7H3007).

[1] R. A. Street, in *Technology and Applications of Amorphous Silicon*, edited by R. A. Street, Springer Series in Materials Science Vol. 37 (Springer, Berlin, 2000), Chap. 4, p. 147.
[2] G. Yu, G. Srdanov, J. Wang, H. Wang, Y. Cao, and A. J. Heeger, Synth. Met. **111**, 133 (2000).
[3] See for example, T. R. Hebner, C. C. Wu, D. Marcy, M. H. Lu, and J. C. Sturm, Appl. Phys. Lett. **72**, 519 (1998).
[4] M. Mulato, F. Lemmi, R. Lau, J-P. Lu, J. Ho, S. E. Ready, J. T. Rahn, and R. A. Street, Proc. SPIE **3977**, 26 (2000).
[5] D. M. Pai, J. F. Yanus, and M. Stolka, J. Phys. Chem. **88**, 4714 (1984).
[6] K. Hecht, Z. Phys. **77**, 235 (1932).
[7] Z. D. Popovic, A-M. Hor, and R. O. Loutfy, Chem. Phys. **127**, 451 (1988).
[8] H. Fujieta, IEEE Trans. Med. Imaging **11**, 34 (1992).
[9] M. Mulato, S. Ready, K. Van Schuylenbergh, J. P. Lu, and R. A. Street, J. Appl. Phys. **89**, 8193 (2001).